AMERICAN SOCIETY FOR MICROBIOLOGY | Antimicrobial Agents and Chemotherapy

Antitubercular Agent Delamanid and Metabolites as Substrates and Inhibitors of ABC and Solute Carrier Transporters

Hiroyuki Sasabe,[a] Yoshihiko Shimokawa,[a] Masakazu Shibata,[a] Kenta Hashizume,[b] Yusuke Hamasako,[b] Yoshihiro Ohzone,[b] Eiji Kashiyama,[a] Ken Umehara[a]

Tokushima Research Institute, Otsuka Pharmaceutical Co., Ltd., Tokushima, Japan[a]; ADME & Toxicology Research Institute, Sekisui Medical Co., Ltd., Ibaraki, Japan[b]

Delamanid (Deltyba, OPC-67683) is the first approved drug in a novel class of nitro-dihydro-imidazooxazoles developed for the treatment of multidrug-resistant tuberculosis. Patients with tuberculosis require treatment with multiple drugs, several of which have known drug-drug interactions. Transporters regulate drug absorption, distribution, and excretion; therefore, the inhibition of transport by one agent may alter the pharmacokinetics of another, leading to unexpected adverse events. Therefore, it is important to understand how delamanid affects transport activity. In the present study, the potencies of delamanid and its main metabolites as the substrates and inhibitors of various transporters were evaluated *in vitro*. Delamanid was not transported by the efflux ATP-binding cassette (ABC) transporters P-glycoprotein (P-gp; MDR1/ABCB1) and breast cancer resistance protein (BCRP/ABCG2), solute carrier (SLC) transporters, organic anion-transporting polypeptides, or organic cation transporter 1. Similarly, metabolite 1 (M1) was not a substrate for any of these transporters except P-gp. Delamanid showed no inhibitory effect on ABC transporters MDR1, BCRP, and bile salt export pump (BSEP; ABCB11), SLC transporters, or organic anion transporters. M1 and M2 inhibited P-gp- and BCRP-mediated transport but did so only at the 50% inhibitory concentrations (M1, 4.65 and 5.71 μmol/liter, respectively; M2, 7.80 and 6.02 μmol/liter, respectively), well above the corresponding maximum concentration in plasma values observed following the administration of multiple doses in clinical trials. M3 and M4 did not affect the activities of any of the transporters tested. These *in vitro* data suggest that delamanid is unlikely to have clinically relevant interactions with drugs for which absorption and disposition are mediated by this group of transporters.

Tuberculosis (TB) is still a serious health problem and a leading cause of death worldwide, with approximately 9.6 million people developing active TB and 1.5 million dying from TB in 2014 alone (1). The current TB treatments are long and burdensome, requiring multidrug chemotherapy typically consisting of rifampin, isoniazid, ethambutol, and pyrazinamide administered under clinical observation (1). TB treatment is further complicated by the emergence of multidrug-resistant TB (MDR-TB) caused by strains of *Mycobacterium tuberculosis* resistant to at least the first-line drugs isoniazid and rifampin and by frequent coinfection with human immunodeficiency virus (HIV)/AIDS. In 2014, it is estimated that 3.3% of all new TB cases and 20% of all previously treated TB cases globally had MDR-TB (1, 2), and the number of TB cases coinfected with HIV is estimated to be 1.2 million, accounting for 12% of the 9.6 million people who developed TB worldwide (1). However, the number of HIV-positive TB patients on antiretroviral therapy was only approximately 392,000 (equivalent to only 33% of the TB patients estimated to be coinfected with HIV) (1). Patients with MDR-TB must be treated for at least 20 months with a combination containing second-line drugs and several antibiotics (quinolones, macrolides, etc.) that are less effective, more expensive, and more toxic than first-line drugs. Consequently, new chemotherapy interventions that can shorten the total treatment duration, provide improved efficacy against MDR-TB, and be administered safely with other antitubercular regimen drugs as well as antiretroviral agents are urgently needed.

In response to this increasing MDR-TB prevalence and the concomitant need for new chemotherapies, Otsuka Pharmaceutical Co., Ltd. (Tokyo, Japan), developed the nitro-dihydro-imidazooxazole derivative delamanid (Deltyba, OPC-67683;(*R*)-2-methyl-6-nitro-2-[(4-{4-[4-(trifluoromethoxy)phenoxy]-piperidin-1-yl}phenoxy)methyl]-2,3-dihydroimidazo [2,1-*b*]oxazole) (3). Delamanid potently inhibits the synthesis of mycolic acid, a long-chain fatty acid of the *M. tuberculosis* cell wall. It demonstrated potent preclinical *in vitro* and *in vivo* activity against both drug-susceptible strains and strains resistant to first-line drugs (4). Clinically, delamanid was demonstrated to have efficacy against *M. tuberculosis* and a favorable safety profile in both drug-sensitive TB patients and MDR-TB patients (5, 6). The agent has received regulatory approval for the treatment of MDR-TB in the European Union, Japan, and the Republic of Korea and is awaiting approval in other regions. A major aim of clinical evaluations has been to determine whether delamanid could help address the unmet needs in TB treatment, including for patients coinfected with HIV and patients with AIDS. However, the introduction of new agents to multidrug regimens for the treatment o fMDR-TB and *M. tuberculosis*-HIV coinfection can generate unexpected drug-drug interactions (DDIs). Although DDIs involve multiple mechanisms, the effects on drug transporters and metabolic pathways (e.g., the effects on cytochrome P450 [CYP] enzymes) are common sources of clinically significant adverse events.

Received 23 December 2015 **Returned for modification** 26 January 2016
Accepted 17 March 2016

Accepted manuscript posted online 28 March 2016

Citation Sasabe H, Shimokawa Y, Shibata M, Hashizume K, Hamasako Y, Ohzone Y, Kashiyama E, Umehara K. 2016. Antitubercular agent delamanid and metabolites as substrates and inhibitors of ABC and solute carrier transporters. Antimicrob Agents Chemother 60:3497–3508. doi:10.1128/AAC.03049-15.

Address correspondence to Hiroyuki Sasabe, Sasabe.Hiroyuki@otsuka.jp.

Supplemental material for this article may be found at http://dx.doi.org/10.1128/AAC.03049-15.

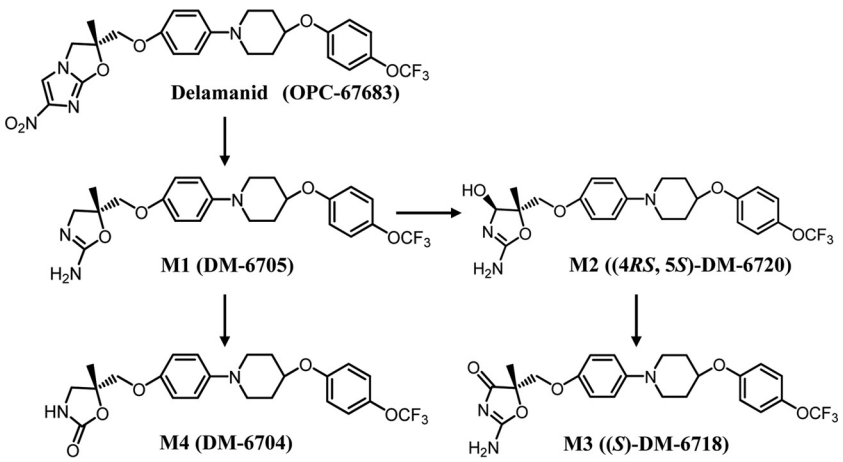

FIG 1 Proposed metabolic pathways of delamanid in humans.

A multitude of drug efflux and uptake transporters is expressed in the intestinal epithelium, liver, kidney, vascular endothelium, and brain, where they regulate the absorption, distribution, and excretion of drugs (7). These transporters are sometimes major determinants of the dispositional fate of drugs, including antibiotics commonly used in the treatment of infections (8, 9). For example, in the process of absorption into the body, fluoroquinolones and β-lactams are predominantly absorbed via organic anion-transporting polypeptides (OATPs) and peptide transporter 1 on the intestinal membrane barrier (8–10). In contrast, there are several reports that fluoroquinolones absorbed into enterocytes are expelled by the ATP-binding cassette (ABC) drug efflux transporter P-glycoprotein (P-gp; MDR1/ABCB1) and breast cancer resistance protein (BCRP/ABCG2) back into the gut lumen (11). The β-lactam antibiotics are substrates for organic anion transporters (OATs) that mediate uptake through the renal basolateral membrane into proximal tubular cells and ultimately into the nephron lumen for excretion (12). The P-gp and BCRP efflux transporters are also expressed in the liver, kidney, mammary gland, and other organs, where they export xenobiotic compounds out of the cell (7, 13). Moreover, P-gp and BCRP limit the penetration of lipophilic compounds through the blood-brain barrier (BBB) and have been reported to transport or interact with macrolides and fluoroquinolones (8, 11, 14, 15).

It is common for an antibiotic to be concomitantly administered with other drugs, including other antibiotics, to improve the overall treatment response. Intestinal absorption, hepatic metabolism, and elimination by renal or biliary excretion involve multiple transporter types; therefore, there is great potential for unforeseen interactions when a newly developed antibiotic is concomitantly used with such substrates and inhibitors of transporters. For instance, rifampin and macrolide antibiotics are potent inhibitors of the human OATP family that mediate the uptake of 3-hydroxy-3-methylglutaryl-coenzyme A reductase inhibitors (statins) of other common drugs (16, 17). These antibiotic agents also have the potential to cause DDIs by inhibiting hepatic uptake of other antibiotics, such as β-lactams and quinolones. In addition, ethambutol also has the ability to inhibit organic cation transporters (OCTs), which are involved in the hepatic or renal uptake of cationic compounds (18). In addition, rifampin can influence drug elimination via CYP3A4 induction. Erythromycin can inhibit the function of P-gp, resulting in an increased absorption of fexofenadine, in addition to its effects on CYP3A (19). Antiretroviral agents that may be used to treat HIV coinfection can also influence the pharmacokinetics and clinical effects of other drugs (20, 21, 40). Therefore, there is an urgent need for a careful *in vitro* characterization of these potential DDIs and, if warranted, assessment of the possible clinical consequences of these DDIs.

In addition to transporter-mediated interactions, DDIs may arise from effects on drug-metabolizing enzymes. When delamanid is orally administered to humans and animals, at least four metabolites are detected in plasma: the primary (*R*)-2-amino-4,5-dihydrooxazole derivative, metabolite 1 (M1; DM-6705); its subsequent oxidative metabolites, the (4*RS*,5*S*)-2-amino-4,5-dihydro-4-hydroxyoxazole derivative [metabolite 2 (M2); (4*RS*,5*S*)-DM-6720] and the (*S*)-2-imino-oxazolidin-4-one derivative [metabolite 3 (M3); (*S*)-DM-6718]; and its hydrolysis metabolite, the (*R*)-4,5-dihydro-2-oxooxazole derivative (metabolite 4 [M4]; DM-6704) (Fig. 1) (22). Delamanid is not metabolized by NADPH-dependent reactions, including those catalyzed by CYP enzymes, in human or animal liver microsomes (4). Also, delamanid was not found to have inhibitory effects on the metabolism of exogenous CYP substrate compounds by eight CYP isoforms (CYP1A2, CYP2A6, CYP2B6, CYP2C8/9, CYP2C19, CYP2D6, CYP2E1, and CYP3A), even at a concentration of 100 μmol/liter, well above the therapeutic concentration (23). The delamanid metabolites were noted to inhibit some other CYP isoforms but only at concentrations much higher than those observed in human plasma after the administration of therapeutic doses. These results indicate that delamanid poses no serious risk for metabolic DDIs.

Thus, in the present study, we focused on delamanid and its four metabolites as the substrates and inhibitors of various drug transporters. We conducted a series of *in vitro* tests in recombinant cell culture systems and membrane vesicles expressing transporters known to influence the pharmacokinetics of other compounds used for TB treatment, including ABC transporters (P-gp, BCRP, bile salt export pump [BSEP]), solute carrier (SLC) transporters, OATPs, OATs, and OCTs.

MATERIALS AND METHODS

Chemicals and reagents. [*dihydroimidazooxazole*-3-^{14}C]delamanid ([^{14}C]delamanid) was synthesized by Quotient Bioresearch (Cardiff, United Kingdom). Delamanid and the four delamanid metabolites, M1 to M4, were synthesized by Otsuka Pharmaceutical Co., Ltd. (Tokyo, Japan). [^{3}H]digoxin, [^{3}H]prazosin, [^{14}C]mannitol, [6,7-^{3}H(N)]estrone 3-sulfate ammonium salt, ([^{3}H]E3S), [6,7-^{3}H(N)]estradiol 17β-D-glucuronide ([^{3}H]$E_2$17βG), and [^{3}H(G)]taurocholic acid ([^{3}H]TCA) were purchased from PerkinElmer (Waltham, MA). *p*-[*glycyl*-2-^{3}H]aminohippuric acid ([^{3}H]PAH) and [*biguanidine*-^{14}C]metformin hydrochloride ([^{14}C]metformin) were purchased from American Radiolabeled Chemicals (St. Louis, MO) and Moravek Biochemicals (Brea, CA), respectively. Other chemicals were obtained from the following sources. Digoxin, PAH, E3A sodium salt, sodium TCA, verapamil, probenecid, rifampin, anhydrous quinidine, and cyclosporine were purchased from Sigma-Aldrich (St. Louis, MO). $E_2$17βG sodium salt and Ko143 were purchased from Santa Cruz Biotechnology (Dallas, TX) and Tocris Bioscience (Bristol, United Kingdom), respectively. All reagents and solvents were of analytical or high-performance liquid chromatography (HPLC) grade, the highest grade, or an equivalent grade.

LLC-PK1 cells expressing MDR1 or BCRP. Porcine kidney epithelial LLC-PK1 cells transfected with vectors containing human MDR1 cDNA and control LLC-PK1 cells transfected with vector only were used under a license from BD Biosciences (Franklin Lakes, NJ). LLC-PK1 cells transfected with vectors containing human BCRP cDNA were developed at the ADME & Toxicology Research Institute, Sekisui Medical Co., Ltd. (Tokyo, Japan).

Prior to the experiments, the cells were cultured in 75-cm^2 flasks and subjected to passage every 3 to 5 days. Cells expressing MDR1 (or the empty vector) were seeded at 4×10^4 cells/insert and cells expressing BCRP (or the empty vector) were seeded at 2.5×10^4 cells/insert in 24-well transwell plates (0.3-cm^2 polyethylene terephthalate porous filter culture inserts with a pore size of 3 μm for MDR1-expressing cells or a pore size of 0.4 μm for BCRP-expressing cells; cell culture insert 24-well companion plate; BD Falcon, Bedford, MA). Seeded MDR1-expressing LLC-PK1 cells were incubated for 8 to 9 days and BCRP-expressing LLC-PK1 cells were incubated for 7 to 8 days in a CO_2 incubator (37°C, 5% CO_2) to prepare cell monolayers for the determination of cellular transport activity. The medium in the flasks and plates containing MDR1-expressing cells was changed every 2 or 3 days, and the medium in the flasks and plates containing BCRP-expressing cells was changed every 2 to 5 days. The medium used for passage in flasks was composed of medium 199 containing 9% fetal bovine serum (FBS), 50 μg/ml gentamicin, and 100 μg/ml hygromycin B. The medium used for passage in 24-well plates was composed of medium 199 containing 9% FBS and 50 μg/ml gentamicin. The electrical resistance across the cell monolayer was measured prior to the preincubation. The electrical resistances were 303 to 714 Ω cm^2 for MDR1-expressing cells and 138 to 474 Ω cm^2 for BCRP-expressing and control cells; these values are within the acceptable range (100 to 800 Ω cm^2).

HEK293 cells expressing OATPs and OCTs. Human embryonic kidney 293 (HEK293) cells transfected with a vector containing human OATP1B1, OATP1B3, OCT1, or OCT2 cDNA and control HEK293 cells transfected with the vector only were developed at Sekisui Medical Co., Ltd. Prior to the experiments, the cells were cultured in 75-cm^2 flasks and subjected to passage every 3 to 5 days. The OATP1B1- and OATP1B3-expressing and control cells were seeded at 3.0×10^5 cells/well in 24-well plates coated with collagen I from rat tail (BD Falcon) and incubated in a CO_2 incubator (37°C, 5% CO_2) for 1 day. The cells were further incubated for 1 day in 0.5 ml of the same medium plus 10 mmol/liter butyric acid. The OCT1- and OCT2-expressing and control cells were seeded at 2.5×10^5 cells/well in the same medium on 24-well plates coated with collagen I and incubated in a CO_2 incubator (37°C, 5% CO_2) for 2 days. The medium was composed of Dulbecco's modified Eagle medium (DMEM) containing 9% FBS, antibiotic-antimycotic, and 2 mmol/liter L-glutamine.

Renal proximal tubule (S2) cells expressing OATs. Cells derived from the second segment of the proximal tubule of transgenic mice harboring the temperature-sensitive simian virus 40 large T-antigen gene (here termed S2 cells) and transfected with a vector including human OAT1 or OAT3 cDNA as well as control S2 cells transfected with the vector were established by Fuji Biomedix Co., Ltd. (Tokyo, Japan), and the cells were succeeded and owned by Sekisui Medical Co., Ltd. Prior to the experiments, OAT1- and OAT3-expressing S2 cells and the corresponding control cells were cultured in 75-cm^2 flasks and subjected to passage every 2 or 4 days. The cells were seeded at 2.5×10^5 or 4×10^5 cells/well in 24-well plates coated with collagen I from newborn bovine skin (Corning, Tewksbury, MA) and incubated in a CO_2 incubator (33°C, 5% CO_2) for 2 days. The passage and plating medium was composed of RITC80-7 (Research Institute for the Functional Peptides Co., Ltd., Higashine, Yamagata, Japan) containing 5% FBS, 10 ng/ml epidermal growth factor, 0.08 unit/ml insulin, and 10 μg/ml transferrin.

BSEP-expressing vesicles. BSEP-expressing and control Sf9 vesicles were purchased from Solvo Biotechnology (Boston, MA) and stored at −80°C until use.

Transwell transport experiments. In transwell plates, the apical-side volume of MDR1-expressing monolayers was maintained at 100 μl and the basal-side volume was maintained at 600 μl. The apical-side volume of BCRP-expressing monolayers was maintained at 250 μl, and the basal-side volume was maintained at 900 μl. Prior to the flux assays, the medium surrounding both the apical and the basal sides was removed and replaced with equal volumes of bovine serum albumin (BSA)-free Hanks' balanced salt solution (HBSS) (pH 7.4) (for delamanid), 1% BSA-HBSS (for M1) containing 0.2% dimethyl sulfoxide (DMSO; vehicle), or inhibitor solution, as indicated below, and the cells were preincubated at 37°C for 1 h. For [^{14}C]delamanid, a higher donor concentration (5 μmol/liter) was needed to ensure adequate quantitation of the radioactivity on the receiver side. Moreover, for M1, the substrate was examined at a concentration of 3 μmol/liter on the donor side. The concentration of M1 on the receiver side was quantitated using liquid chromatography-tandem mass spectrometry (LC-MS/MS). M1 exhibited adsorption to the membrane filter of the monolayer device, whereas the adsorption of delamanid was negligible. To avoid adsorption, 1% BSA-HBSS containing BSA was used as a transport buffer for M1. The absolute transport in the presence of albumin may be reduced because of the protein binding of the substrate. However, we believe that the transport of M1 for P-gp and BCRP can be evaluated by the ratio of the net flux, defined as the ratio of the permeation clearance for the transporter-expressing cells to that for the control cells.

For the assessment of drug transport from the apical side to the basal side, the apical-side medium was replaced with the test substance as the substrate/inhibitor or with [^{14}C]mannitol solution, and the basal-side medium was replaced with BSA-free HBSS, 1% BSA-HBSS containing 0.2% DMSO, or inhibitor solution, as appropriate. Conversely, for the assessment of transport from the basal side to the apical side, the apical-side medium was replaced with fresh BSA-free HBSS, 1% BSA-HBSS containing 0.2% DMSO, or inhibitor solution, as appropriate, and the basal-side medium was replaced with the test substance as the substrate/inhibitor or [^{14}C]mannitol solution. Then, the cells were incubated at 37°C for designated times (0.25, 0.5, and 1 h for [^{3}H]prazosin and 1, 2, and 4 h or 2, 3, and 4 h for the test compounds, as indicated below). Incubation was conducted in triplicate. At the designated stop time, 70 μl (for MDR) or 100 μl (for BCRP) of the sample on the basal or apical side was collected for the assessment of transport from the apical to the basal side or the basal to the apical side, respectively. The same volume of BSA-free HBSS, 1% BSA-HBSS containing 0.2% DMSO, or inhibitor solution was quickly added to compensate for the sampled volume.

For experiments using radiolabeled substrate and reference compounds, scintillation cocktail (10 ml; Hionic-Fluor; PerkinElmer) was added to the collected samples. For the nonlabeled substance, a 50-μl

aliquot of the collected sample was mixed with BSA-free HBSS or 1% BSA-HBSS (40 μl) and the internal standard solution (10 μl of 500 ng/ml OPC-14714). This mixture was injected directly into an LC-MS/MS system. The detailed treatments are as described below in the description of the LC-MS/MS analysis. The substrate or reference compound concentration in the sample before incubation was measured using a similar procedure.

Cellular uptake experiments. The medium in each seeded well was replaced by fresh HBSS (300 μl), and the cells were preincubated at 37°C for 15 min. Uptake was started by replacement of the free HBSS with the substrate solution or substrate solution containing an inhibitor. Both the [^{14}C]delamanid and M1 concentrations were set to 3 μmol/liter. The uptake reaction was performed in triplicate at 37°C for each designated time (1, 2, and 5 min for OATPs and 2, 5, and 10 min for OCT1). The substrate solution was then removed, and the cells were washed once with 1 ml of ice-cold phosphate-buffered saline (PBS) containing 0.2% BSA and twice with 1 ml of ice-cold PBS. The intracellular fraction was isolated as described below.

For the radiolabeled substrate, after PBS was removed, 0.1 mol/liter NaOH (0.5 ml) was added to each well and the contents of the wells were mixed thoroughly by pipetting to dissolve the cells. An aliquot (0.3 ml) of the cell lysate was mixed with the scintillation cocktail (10 ml; Hionic-Fluor). For the nonlabeled substrate, after PBS was removed, PBS containing 0.1% DMSO (0.5 ml) was added and the contents of the wells were mixed thoroughly by pipetting to suspend the cells. An aliquot (50 μl) of the cell suspension was mixed with PBS (40 μl) and the internal standard solution (10 μl). This solution was injected into an LC-MS/MS system. The substrate or reference compound concentration in the sample before incubation was measured using a similar procedure. The uptake volume was calculated on the basis of the amount in the lysate and the concentration observed before incubation.

Vesicular uptake experiments. Prior to incubation, glass fiber filters (MultiScreen HTS FB fast-flow-rate-type glass fiber filters; pore size, 1.0 μm; Merck, Kenilworth, NJ) in culture wells were washed once with a solution of 10 mmol/liter Tris-HCl, 100 mmol/liter KNO_3, 50 mmol/liter sucrose, and 100 μmol/liter TCA. The filters were then left for at least 30 min in 0.1% BSA solution (200 μl/well). After removal of the 0.1% BSA solution by aspiration, the filters were washed twice again with the washing solution.

BSEP-expressing or control vesicles were preincubated at 37°C for 5 min in a reaction buffer consisting of 2 mmol/liter HEPES-Tris, 100 mmol/liter KNO_3, 10 mmol/liter $Mg(NO_3)_2$, and 50 mmol/liter sucrose plus substrate or inhibitor. Then, a 20-μl aliquot of a 10-mmol/liter Mg-ATP solution was added to start the uptake reaction, which was allowed to proceed at 37°C for 5 min. All incubations were conducted in triplicate. At the times designated below, ice-cold washing solution (200 μl) was added to terminate the reaction. An aliquot (200 μl) of each mixture was passed through a glass fiber filter by aspiration. Loaded filters were washed five times with 200 μl ice-cold washing solution, transferred to a vial, and mixed with 0.5 ml ethanol and 5 ml scintillation cocktail (Ultima Gold; PerkinElmer) for measurement of the amount of intravesicular substrate. An aliquot of the remaining reaction mixture (30 μl) was mixed with 5 ml of scintillation cocktail (Ultima Gold) for measurement of the amount of extravesicular substrate remaining.

LC-MS/MS analysis of M1. Ice-cold methanol (200 μl) was added to each assay sample. The mixture was stirred for approximately 20 s using a vortex mixer and centrifuged (16,000 × *g*, 4°C, 5 min). The supernatant (0.25 ml) was collected, and ice-cold water-formic acid (50:1, vol/vol; 180 μl) was added. This mixture was stirred for approximately 10 s using a vortex mixer and filtered through a membrane (pore size, 0.2 μm; W-MO; Kurabo, Osaka, Japan) by centrifugation (2,200 × *g*, 4°C, 5 min). The obtained filtrate was injected directly into the LC-MS/MS system.

LC-MS/MS analysis was conducted using an API4000 MS system (AB Sciex, Framingham, MA) connected to an LC20 series HPLC system (Shimadzu, Kyoto, Japan). Chromatographic separation was achieved on a Capcell Pak MGII C_{18} column (particle size, 3 μm; 2.0 mm [inside diameter] by 50 mm; Shiseido, Tokyo, Japan) using mixtures of two solvents, solvent A (1 mmol/liter ammonium formate aqueous solution and formic acid [1,000:2, vol/vol]) and solvent B (methanol), at a constant flow rate of 0.25 ml/min. The elution steps were as follows: 0 to 1.0 min of a linear gradient of from 25% to 40% solvent B, 1.0 to 9.0 min of a linear gradient of from 40% to 55% solvent B, and 9.0 to 13.0 min of an isocratic elution at 55% solvent B. Equilibration was achieved 8 min after returning to the initial conditions. The column effluent was delivered to the electrospray ionization ion source in positive ion multiple-reaction-monitoring mode to produce product ions of *m*/*z* 466.5 → 352.0 for M1 and *m*/*z* 458.2 → 295.5 for the internal standard (OPC-14714, a benzoquinolinone analogue compound used in the quantitation method involving human plasma [24]). The calibration of M1 both in 1% BSA-HBSS and in the cell suspension showed good linearity (correlation coefficient [*r*], 0.9976 to 0.9983 and 0.9958 to 0.9984, respectively) over the M1 concentration range of 1.2 to 1,200 nmol/liter using weighted (1/concentration^2) least-squares regression. The lower limit of qualification (LLOQ), defined as the lowest concentration measurable on the calibration curve, was 1.2 nmol/liter. The precision included the LLOQ and ranged from 2.7% to 13.0% in 1% BSA-HBSS and from 2.0% to 8.4% in the cell suspension. The intrabatch accuracy included the LLOQ and ranged from −8.5% to 3.9% in 1% BSA-HBSS and from −3.0% to 11.6% in the cell suspension. The specificity at the LLOQ was 12.1% in 1% BSA-HBSS and 0.0% in the cell suspension, and the postpreparative stability ranged from 94.0% to 112.0% and from 88.7% to 100.4% in 1% BSA-HBSS and in the cell suspension, respectively. These results met the corresponding criteria for the determination of M1.

Protein content assay. The protein content in the cell lysate was assayed using the a bicinchoninic acid protein assay kit (Thermo Fisher Scientific, Waltham, MA). Briefly, 20 μl of each cell lysate sample or BSA calibration solution (0, 0.05, 0.1, 0.25, 0.5, and 0.75 mg protein/ml) was aliquoted, the aliquots were placed in 96-well plates, and 200 μl of the kit reagent mixture was added to each well. The mixtures were incubated at 37°C for 30 min, and the absorbance at 562 nm was measured on a microplate reader (HT; DS Pharma Biomedical, Osaka, Japan). Incubation was performed in duplicate.

Measurement of radioactivity. The radioactivity in each sample was measured over 2 min using a liquid scintillation counter (LSC; 2500TR, 3100TR, or 1900CA; PerkinElmer). The counting efficiency was corrected by the external standard source method. The detection limit of the radioactivity was defined as the background radioactivity.

Calculation of parameters. In the cell monolayer experiments using MDR1-expressing and BCRP-expressing LLC-PK1 cells, the permeation volume and clearance were calculated from the amounts that permeated across transporter-expressing or control cell monolayers and the initial concentration, according to the following equations: permeation volume = permeated amount (amount per well)/initial concentration (amount per microliter) and permeation clearance ratio = basal side-to-apical side permeation clearance/apical side-to-basal side permeation clearance (where clearance is in microliters per well per hour), where permeation clearance was determined by linear regression of the permeation volume and the incubation time. Further, the ratio of the permeation clearance for transporter-expressing cells to that for control cells was defined as the net flux ratio. In the uptake experiments using HEK293 or S2 cells expressing OATs, OCTs, or OATPs, the uptake volume was calculated from the amount of substrate in the cell lysate and the initial substrate concentration according to the following equation: uptake volume (in microliters per milligram of protein) = uptake amount (in amount per well)/protein content (in milligrams of protein per well) × initial concentration (in amount per microliter).

Further, the ratio of the uptake volume for transporter-expressing cells to that for control cells was defined as the uptake ratio. In the vesicle experiment, the uptake amount and protein content were expressed per tube.

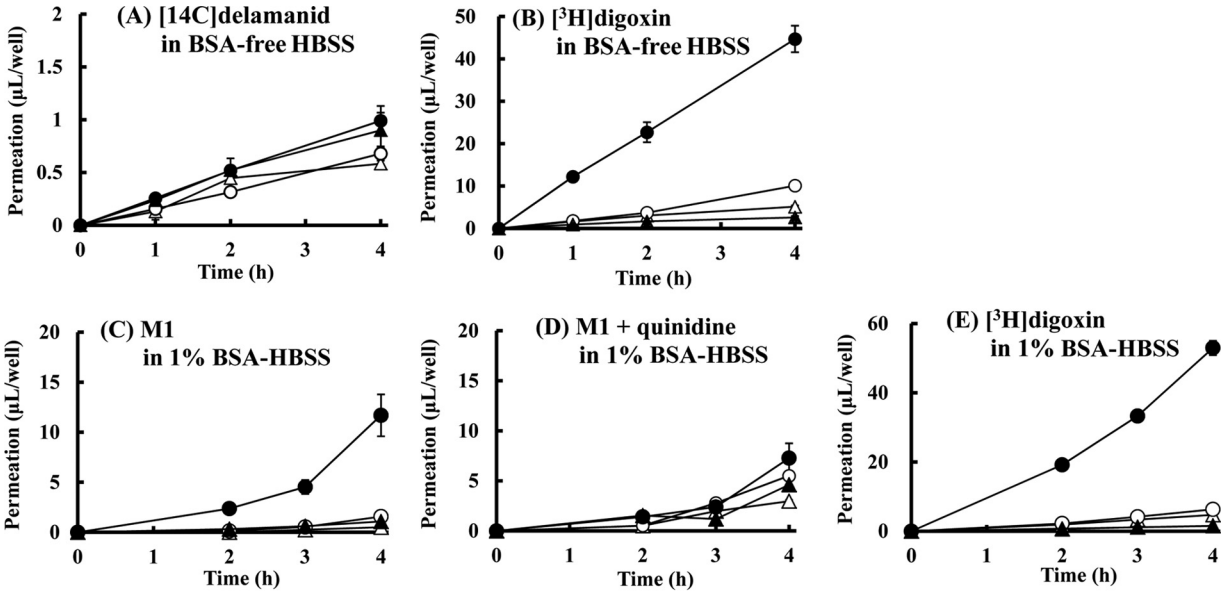

FIG 2 Time profiles for the transcellular transport of [^{14}C]delamanid and metabolite M1 across control LLC-PK1 cells (open symbols) and MDR1-expressing LLC-PK1 cells (closed symbols). The experiment was started by the addition of the following substrate to one compartment: [^{14}C]delamanid (5 μmol/liter) in BSA-free HBSS (A), [^{3}H]digoxin (1 μmol/liter) in BSA-free HBSS (B), M1 (3 μmol/liter) in 1% BSA-HBSS (C), M1 (3 μmol/liter) plus quinidine (30 μmol/liter) in 1% BSA-HBSS (D), or [^{3}H]digoxin (1 μmol/liter) in 1% BSA-HBSS (E). The inhibitor quinidine was added in both the apical and basal compartments. Circles, basal side-to-apical side flux; triangles, apical side-to-basal side flux. Data are expressed as the mean ± SD from triplicate determinations.

In the experiments measuring the inhibition of monolayer permeation, the remaining activity (as a percentage of that for the control) was determined as the ratio of the net flux in the presence and absence of an inhibitor as follows: remaining activity as a percentage of that for the control = (net flux ratio in the presence of inhibitor/net flux ratio in the absence of inhibitor) × 100.

In the uptake inhibition experiments, the remaining activity was calculated according to the following equation: remaining activity as a percentage of that for the control = (uptake volume in transporter-expressing cells − control cells in the presence of inhibitor)/(uptake volume in transporter-expressing cells − control cells in the absence of inhibitor) × 100.

In the monolayer permeation experiment, the 50% inhibitory concentration (IC_{50}) was calculated by the maximum inhibitory effect (I_{max}) equation, using WinNonlin software (version 6.1; Pharsight Corporation), as follows: net flux ratio in the presence of inhibitor/net flux ratio in the absence of inhibitor = $1 - (I_{max} \times I^C)/(I^C + IC_{50}{}^C)$, where I is the inhibitor concentration and C is the Hill coefficient.

When the remaining activity as a percentage of the activity of the control at the maximum concentration tested was greater than 50.0%, the IC_{50} was indicated to be greater than the maximum concentration. All data on transport kinetics are expressed as the mean ± standard deviation (SD) from triplicate determinations.

Assessment of risk of DDIs. For the purpose of clinical DDIs, the values of the maximum total plasma concentration (free and bound) (C_{max})/IC_{50} and 50 times the maximum free (unbound) plasma concentration ($C_{max,u}$)/IC_{50} [(50 × $C_{max,u}$)/IC_{50}] when 100 mg delamanid was administered twice per day were calculated for assessment of the risk for compounds that had an IC_{50} for any transporter (22). IC_{50} is the value obtained in the present study. The free fraction of M1 is reported to be 0.003 (22), and that of M2 is assumed to be equivalent to that of M1 because the chemical structures and physiological properties of M1 and M2 are similar.

RESULTS

Delamanid transport across cell monolayers expressing the ATP-binding cassette transporter P-gp/MDR1 or BCRP. Cell monolayer flux experiments indicated that delamanid is not a substrate for the P-gp/MDR1 efflux transporter. The permeation clearance of [^{14}C]delamanid at 5 μmol/liter across MDR1-expressing LLC-PK1 cell monolayers was 0.233 μl/well/h from the apical to the basal side and 0.251 μl/well/h from the basal to the apical side, and the permeation clearance ratio was 1.1. This was only slightly greater than that across control LLC-PK1 cell monolayers, which was 0.160 μl/well/h from the apical to the basal side and 0.167 μl/well/h from the basal to the apical side and for which the clearance ratio was 1.0, indicating no specific flux direction (Fig. 2A). In contrast, the permeation clearance of M1 at 3 μmol/liter across MDR1-expressing cell monolayers was 0.235 μl/well/h from the apical to the basal side and 2.25 μl/well/h from the basal to the apical side and the permeation clearance ratio was 9.6, while the permeation clearance across control cell monolayers was 0.0965 μl/well/h from the apical to the basal side and 0.284 μl/well/h from the basal to the apical side and the permeation clearance ratio was 2.9 (Fig. 2C). The presence of the P-gp inhibitor quinidine decreased the permeation clearance ratio of M1 by 1.6 across the MDR1-expressing cell monolayers and by 1.7 across the control cell monolayers (Fig. 2D). The net flux ratio of M1 was 3.3, which disappeared in the presence of quinidine. Thus, unlike delamanid, M1 is a substrate for P-gp/MDR1.

Delamanid was also not transported by BCRP. The permeation clearance of [^{14}C]delamanid across BCRP-expressing LLC-PK1 cell monolayers was 0.536 μl/well/h from the apical to the basal side and 0.647 μl/well/h from the basal to the apical side and the permeation clearance ratio was 1.2 (Fig. 3A). These values are close to those for permeation clearance across control LLC-PK1 cells, which was 0.568 μl/well/h from the apical to the basal side and 0.616 μl/well/h from the apical to the basal side, and the permeation clearance ratio of 1.1 for control LLC-PK1 cells was similar to that for BCRP-expressing LLC-PK1 cells (Fig. 3A).

In contrast to the findings for MDR1, M1 was not a substrate

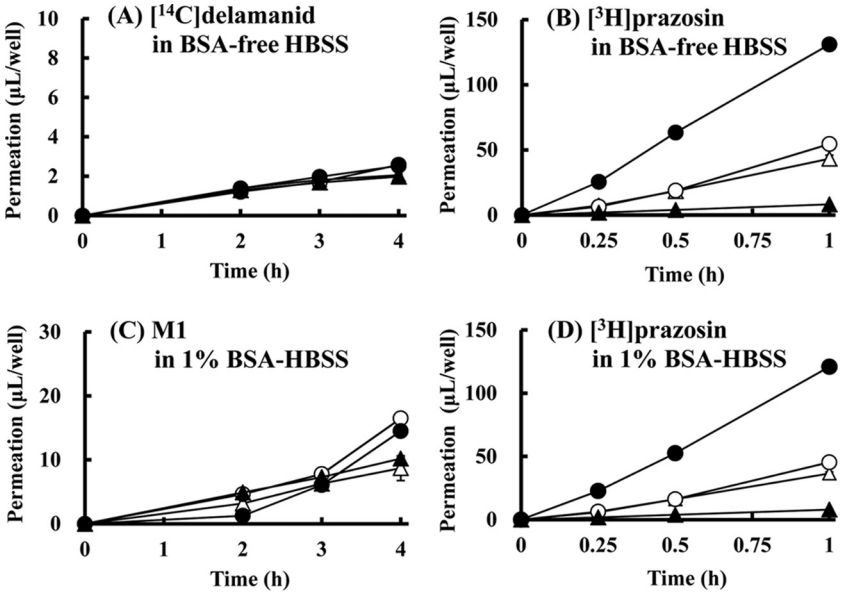

FIG 3 Time profiles of [^{14}C]delamanid and metabolite M1 transport across control LLC-PK1 cells (open symbols) and BCRP-expressing LLC-PK1 cells (closed symbols). The experiment was started by the addition of the following substrate: [^{14}C]delamanid (5 μmol/liter) in BSA-free HBSS (A), [^{3}H]prazosin (0.01 μmol/liter) in BSA-free HBSS (B), M1 (3 μmol/liter) in 1% BSA-HBSS (C), or [^{3}H]prazosin (0.01 μmol/liter) in 1% BSA-HBSS (D). Circles, basal side-to-apical side flux; triangles, apical side-to-basal side flux. Data are expressed as the mean ± SD from triplicate determinations.

for BCRP. The permeation clearance of M1 across BCRP-expressing LLC-PK1 cell monolayers was 2.51 μl/well/h from the apical to the basal side and 2.72 μl/well/h from the basal to the apical side and the permeation clearance ratio was only 1.1, while the permeation clearance of M1 across the control cells was 2.07 μl/well/h from the apical to the basal side and 3.41 μl/well/h from the basal to the apical side and the permeation clearance ratio was 1.6 (Fig. 3C). The permeation clearance ratio of the known BCRP substrate [^{3}H]prazosin was significantly greater than that for the control cells, with the net flux ratio ranging from 12.3 to 13.3 (Fig. 3B and D). Thus, compared to the findings for [^{3}H]prazosin, neither delamanid nor M1 was transported in significant amounts by BCRP.

Uptake transport of delamanid and M1 by OATPs and OCT1. The uptake ratio of the known OATP substrate [^{3}H]$E_2$17βG was 416.0 at 5 min for HEK293 cells expressing OATP1B1 and 96.2 at 5 min for HEK293 cells expressing OATP1B3 (Fig. 4C), indicating substantial functional uptake activity in these cells. However, the delamanid and M1 uptake ratios were only slightly larger than those for control cells (Fig. 4A and

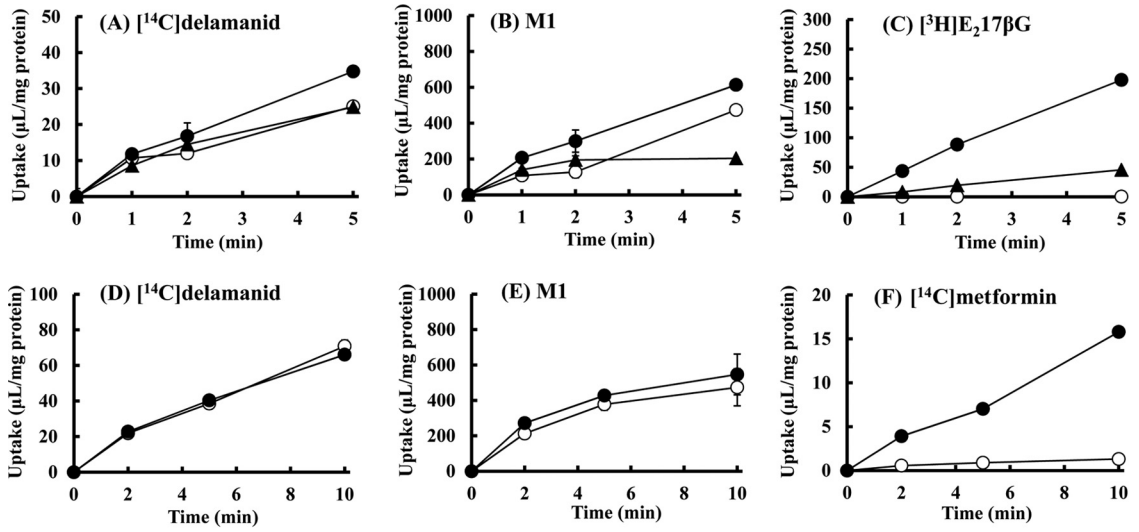

FIG 4 Time profiles of [^{14}C]delamanid and metabolite M1 uptake into control HEK293 cells (open symbols) and OATP-expressing (A to C) or OCT1-expressing (D to F) HEK293 cells (closed symbols). The experiment was started by the addition of the following substrate in BSA-free HBSS: [^{14}C]delamanid (1 μmol/liter) (A and D), M1 (1 μmol/liter) (B and E), or [^{3}H]$E_2$17βG (0.05 μmol/liter) (C and F). Circles in panels A to C, OATP1B1; triangles in panels A to C, OATP1B3. Data are expressed as the mean ± SD from triplicate determinations.

TABLE 1 Inhibitory effects of delamanid and its metabolites on the MDR1-mediated transport of [^{3}H]digoxin and BCRP-mediated transport of [^{3}H]prazosin[a]

Concn (μmol/liter)	% remaining for MDR1-mediated transport					% remaining for BCRP-mediated transport				
	Delamanid	M1	M2	M3	M4	Delamanid	M1	M2	M3	M4
0.03	106.0	—[b]	—	92.0	106.6	—	—	—	76.0	88.0
0.1	119.1	91.7	87.0	92.0	101.7	82.7	104.4	92.6	85.3	85.3
0.3	99.0	78.5	87.7	90.1	100.0	74.7	92.6	86.8	77.3	82.7
1	123.4	94.2	90.1	69.1	122.3	93.3	95.6	86.8	72.0	68.0
3	109.2	73.6	95.7	71.0	128.1	80.0	83.8	77.9	61.3	53.3
10 or 5[c]	129.2	24.8	36.4	—	—	86.7	33.8	42.6	—	—
Control[d]	14.2	13.2	9.3	9.3	13.2	17.3	19.1	19.1	17.3	17.3

[a] The transport of [^{3}H]digoxin (1 μmol/liter) and [^{3}H]prazosin (10 nmol/liter) was determined after incubation at 37°C for 2 and 1 h, respectively. At 0 μmol/liter, the ratio of transport from the basal to the apical side to the transport from the apical to the basal side was as follows (the data represent the ratio for transporter-expressing LLC-PK1 cells/the ratio for transporter-nonexpressing LLC-PK1 cells): 13.1/1.4, 16.9/1.4, 21.1/1.3, and 16.9/1.4 for delamanid, M1, M2 and M3, and M4, respectively, for MDR1-mediated transport and 8.2/1.1, 8.1/1.2, and 8.2/1.1 for delamanid, M1 and M2, and M3 and M4, respectively, for BCRP-mediated transport. The values of percent remaining are the ratio of net transport in the presence of inhibitor to that in the absence of inhibitor (concentration, 0 μmol/liter). Each value represents the ratio of the mean permeation rate obtained from triplicate determinations.

[b] —, not tested.

[c] Delamanid metabolites M1 and M2 were incubated at 10 μmol/liter. Delamanid was incubated at 5 μmol/liter because of its low solubility.

[d] The controls were verapamil at 30 μmol/liter for MDR1-mediated transport and Ko143 at 1 μmol/liter for BCRP-mediated transport.

B). Similarly, the uptakes ratios of delamanid and M1 were similar for OATP1B3-expressing and control HEK293 cells, except at 5 min, when the uptake for control cells was actually larger (Fig. 4A and B). Moreover, the uptake profiles of delamanid and M1 were almost identical in the presence of the OATP inhibitor rifampin (10 μmol/liter) (see Fig. S1B in the supplemental material). These results indicate that delamanid and M1 are not substrates of either OATP1B1 or OATP1B3. The reason for the lack of an increase in M1 uptake at 5 min in the OATP1B3-expressing cells remains unclear.

The uptake ratio of the known OCT1 substrate [^{14}C]metformin for OCT1-expressing HEK293 cells was 12.0 at 10 min, which is substantially larger than that for control cells and which indicates functional uptake activity (Fig. 4F). However, the uptake ratios of delamanid and M1 for OCT1-expressing HEK293 cells were either almost the same as or only slightly higher than those for control cells (Fig. 4D and E), and there was no remarkable change in the presence of the OCT inhibitor quinidine (100 μmol/liter; data not shown). These results indicate that delamanid and M1 are not substrates for OCT1.

Inhibition of P-gp and BCRP transport by delamanid and metabolites. Delamanid had no influence on the net efflux ratio of the MDR1 substrate [^{3}H]digoxin or the BCRP substrate [^{3}H]prazosin across LLC-PK1 cell monolayers expressing MDR1 or BCRP at up to 5 μmol/liter, even in their presence on both the apical and basal sides (Table 1). In contrast, M1 and M2 reduced digoxin transport by P-gp but with relatively high IC_{50}s of 4.65 μmol/liter and 7.80 μmol/liter, respectively (Table 1; see Table 6). M1 and M2 also inhibited [^{3}H]prazosin transport by BCRP, with IC_{50}s of 5.71 μmol/liter and 6.02 μmol/liter, respectively (Table 1; see Table 6).

Inhibition of OATP, OAT, and OCT transport by delamanid and metabolites. Similarly to P-gp/MDR1 and BCRP, delamanid (up to 5 μmol/liter) had little effect on the uptake of [^{3}H]$E_2$17βG by OATP1B1 or OATP1B3 expressed in HEK293 cells, [^{3}H]PAH uptake by OAT1 or [^{3}H]E3S uptake by OAT3 expressed in S2 cells, or [^{14}C]metformin uptake by OCT1 or OCT2 expressed in

TABLE 2 Inhibitory effects of delamanid and its metabolites on OATP1B1- and OATP1B3-mediated uptake of [^{3}H]$E_2$17βG[a]

Concn (μmol/liter)	% remaining for OATP1B1-mediated uptake					% remaining for OATP1B3-mediated uptake				
	Delamanid	M1	M2	M3	M4	Delamanid	M1	M2	M3	M4
0.03	—[b]	—	—	103.5	93.7	—	—	—	82.2	102.8
0.1	94.9	106.1	96.6	103.6	97.7	98.9	109.2	97.1	103.0	119.5
0.3	105.6	113.0	106.9	115.0	100.6	102.0	104.1	103.2	93.4	104.7
1	97.0	117.5	112.4	100.8	97.0	102.1	103.0	101.4	96.8	101.6
3	102.1	113.8	108.2	98.2	94.4	97.3	101.5	105.1	91.5	103.9
10 or 5[c]	104.9	111.1	98.1	—	—	100.7	86.9	102.4	—	—
Control[d]	2.9	4.0	4.6	5.3	3.9	0.8	1.7	2.2	0.1	2.8

[a] The uptake volume of [^{3}H]$E_2$17βG (50 nmol/liter) in transporter-nonexpressing cells ranged from 0.501 ± 0.115 to 0.969 ± 0.228 μl/mg protein/2 min (for both the OATP1B1 and OATP1B3 controls). The OATP1B1- and OATP1B3-mediated uptake volumes of [^{3}H]$E_2$17βG in transporter-expressing HEK293 cells minus the corresponding values in transporter-nonexpressing control HEK293 cells were 140 ± 2, 115 ± 11, 147 ± 11, 115 ± 11, and 125 ± 7 μl/mg protein/2 min for delamanid, M1, M2, M3, and M4, respectively, for OATP1B1-expressing cells and 15.5 ± 1.0, 13.9 ± 0.5, 14.8 ± 0.6, 17.2 ± 0.6, and 13.1 ± 0.4 μl/mg protein/2 min for delamanid, M1, M2, M3, and M4, respectively, for OATP1B3-expressing cells. The uptake volumes are the means ± SDs from triplicate determinations. The uptake as the percent remaining is the ratio of the transporter-mediated uptake volume in the presence of inhibitor to that in the absence of inhibitor (concentration, 0 μmol/liter) and is expressed as the mean ± SD from triplicate determinations.

[b] —, not tested.

[c] Delamanid metabolites M1 and M2 were incubated at 10 μmol/liter. Delamanid was incubated at 5 μmol/liter because of its low solubility.

[d] The control was rifampin at 10 μmol/liter.

TABLE 3 Inhibitory effects of delamanid and its metabolites on OAT1-mediated uptake of [^{3}H]PAH and OAT3-mediated uptake of [^{3}H]E3S[a]

Concn (μmol/liter)	% remaining for OAT1-mediated uptake					% remaining for OAT3-mediated uptake				
	Delamanid	M1	M2	M3	M4	Delamanid	M1	M2	M3	M4
0.03	—[b]	—	—	109.0	104.1	—	—	—	116.3	106.5
0.1	91.2	107.5	103.7	121.5	104.3	116.3	87.5	87.1	121.8	102.8
0.3	90.8	118.2	119.8	109.8	97.8	112.3	92.0	92.1	131.9	105.8
1	79.6	116.9	116.5	120.0	89.3	107.8	109.0	105.4	158.3	94.5
3	81.3	116.2	114.4	157.7	84.5	105.4	114.8	101.7	189.2	89.5
10, 5[c]	75.9	107.2	113.1	—	—	114.7	195.2	165.6	—	—
Control[d]	5.9	8.7	11.4	11.3	5.7	6.5	11.1	9.2	7.5	6.6

[a] In transporter-nonexpressing control S2 cells, the uptake volume of [^{3}H]PAH (1 μmol/liter) ranged from 0.636 ± 0.095 to 0.947 ± 0.141 μl/mg protein/2 min and that of [^{3}H]E3S (50 nmol/liter) ranged from 0.874 ± 0.155 to 2.20 ± 0.37 μl/mg protein/2 min. The OAT1- and OAT3-mediated uptake volumes of [^{3}H]PAH and [^{3}H]E3S are the uptake volumes in transporter-expressing cells minus the uptake volumes in the corresponding transporter-nonexpressing cells and were 51.2 ± 4.2, 56.4 ± 8.1, 53.3 ± 5.6, 29.5 ± 1.0, and 44.8 ± 3.5 μl/mg protein/2 min for delamanid, M1, M2, M3, and M4, respectively, for OAT1-expressing cells and 30.5 ± 0.2, 22.8 ± 0.7, 19.8 ± 1.9, 19.5 ± 0.6, and 32.0 ± 0.3 μl/mg protein/2 min for delamanid, M1, M2, M3, and M4, respectively, for OAT3-expressing cells. The uptake volumes are the means ± SDs from triplicate determinations. The uptake as the percent remaining is the ratio of uptake volume in the presence of an inhibitor to that in the absence of the inhibitor (concentration, 0 μmol/liter) and is expressed as the mean ± SD from triplicate determinations.

[b] —, not tested.

[c] Delamanid metabolites M1 and M2 were incubated at 10 μmol/liter. Delamanid was incubated at 5 μmol/liter because of its low solubility.

[d] The control was probenecid at 100 μmol/liter.

HEK293 cells compared to the uptake in the corresponding control cells (Tables 2 to 4). Moreover, the four delamanid metabolites exerted no inhibition of OATPs, OATs, or OCTs, except for the weak inhibition of OCT1-mediated [^{14}C]metformin uptake by M1 at the highest concentration tested (10 μmol/liter) (Tables 2 to 4). The enhancement of OAT1 and OAT3 transport was observed at higher concentrations of M1, M2, and M3 (Table 3). Such an enhancement of transport has been observed less frequently when a highly lipophilic compound is present in an *in vitro* experiment. These lipophilic metabolites may induce a minor conformational change to the transporter protein or influence membrane fluidity.

Inhibition of BSEP vesicular transport. Delamanid and its four metabolites did not inhibit the uptake of the BSEP substrate [^{3}H]TCA into vesicles, as measured by subtracting the ATP-dependent uptake into control vesicles from that into BSEP-expressing vesicles (Table 5).

Assessment of risk of DDIs. M1 and M2 demonstrated inhibitory potency for P-gp and BCRP, and the IC_{50}s were obtained. Therefore, the values of C_{max}/IC_{50} and $(50 \times C_{max,u})/IC_{50}$ were calculated to assess the risk of inhibition. The values of C_{max}/IC_{50} for M1 were 0.07 and 0.06 for P-gp/MDR1 and BCRP, respectively (Table 6). The value of C_{max}/IC_{50} for M2 was 0.02 for both P-gp/MDR1 and BCRP (Table 6). The value of $(50 \times C_{max,u})/IC_{50}$ for both M1 and M2 was less than the value of C_{max}/IC_{50}. The C_{max}/IC_{50} and $(50 \times C_{max,u})/IC_{50}$ values were not obtained for delamanid, M3, and M4 because their potency for transporters was not evident.

DISCUSSION

A substantial proportion of the delamanid absorbed following oral ingestion by humans and animals is thought to be metabolized first by hydrolysis with albumin (25). The predominant delamanid metabolites are subsequently produced through the proposed metabolic pathways shown in Fig. 1 (22). The primary metabolite of delamanid, the (*R*)-2-amino-4,5-dihydrooxazole derivative (M1), subsequently undergoes oxidative biotransformation reactions to the (4*RS*,5*S*)-2-amino-4,5-dihydro-4-hy-

TABLE 4 Inhibitory effects of delamanid and its metabolites on OCT1- and OCT2-mediated uptake of [^{14}C]metformin[a]

Concn (μmol/liter)	% remaining OCT1-mediated uptake					% remaining OCT2-mediated uptake				
	Delamanid	M1	M2	M3	M4	Delamanid	M1	M2	M3	M4
0.03	—[b]	—	—	110.9	103.6	—	—	—	97.3	96.1
0.1	101.5	90.2	84.6	99.4	97.0	88.1	99.6	101.5	116.6	101.6
0.3	86.9	95.9	75.8	100.3	102.9	109.2	105.2	108.3	120.3	102.2
1	99.1	88.0	92.5	109.0	126.0	116.5	101.9	125.1	112.9	86.2
3	130.9	97.7	133.1	136.9	132.9	107.4	92.4	109.6	113.0	87.7
10, 5[c]	117.4	58.4	82.5	—	—	109.6	87.8	100.8	—	—
Control[d]	2.0	2.8	3.7	6.7	8.1	1.3	0.6	1.2	1.3	0.5

[a] The uptake volume of [^{14}C]metformin (10 μmol/liter) in transporter-nonexpressing control HEK293 cells ranged from 0.941 ± 0.046 to 1.08 ± 0.09 μl/mg protein/5 min for the OCT1 control and from 0.478 ± 0.026 to 0.564 ± 0.095 μl/mg protein/2 min for the OCT2 control. The OCT1- and OCT2-mediated uptake volumes of [^{14}C]metformin are the values in transporter-expressing cells minus those in the corresponding control cells and were 4.67 ± 0.29, 5.98 ± 0.16, 4.82 ± 0.28, 3.52 ± 0.19, and 3.69 ± 0.26 for delamanid, M1, M2, M3, and M4, respectively, for OCT1-expressing cells and 66.3 ± 3.4, 66.7 ± 1.1, 69.7 ± 4.9, 72.5 ± 4.9, and 75.6 ± 3.4 for delamanid, M1, M2, M3, and M4, respectively, for OCT2-expressing cells. The uptake volumes are the means ± SDs from triplicate determinations. The uptake as the percent remaining is the ratio of the uptake volume in the presence of the inhibitor to that in the absence of the inhibitor (concentration, 0 μmol/liter) and is expressed as the mean ± SD from triplicate determinations.

[b] —, not tested.

[c] Delamanid metabolites M1 and M2 were incubated at 10 μmol/liter. Delamanid was incubated at 5 μmol/liter because of its low solubility.

[d] The control was quinidine at 100 μmol/liter for OCT1-mediated uptake and quinidine at 300 μmol/liter for OCT2-mediated uptake.

TABLE 5 Inhibitory effects of delamanid and its metabolites on BSEP-mediated vesicular uptake of [^{14}C]TCA[a]

Concn (μmol/liter)	% remaining BSEP-mediated uptake				
	Delamanid	M1	M2	M3	M4
0.03	—[b]	—	—	—	100.7
0.1	95.5	95.2	75.5	103.6	87.7
0.3	100.8	94.9	129.5	81.6	89.6
1	99.0	96.5	113.1	107.9	98.2
3	108.6	107.3	119.4	106.0	92.4
10 or 5[c]	95.7	99.2	127.8	152.0	—
Control[d]	11.1	11.1	22.0	22.0	11.1

[a] The uptake volume of [^{14}C]TCA (2 μmol/liter) in transporter-nonexpressing control vesicles ranged from 17.1 ± 5.8 to 22.9 ± 1.8 μl/mg protein/5 min. The BSEP-mediated uptake volume of [^{14}C]TCA is the value in BSEP-expressing vesicles minus that in BSEP-nonexpressing control vesicles and was 77.5 ± 11.2 μl/mg protein/5 min for delamanid and M1, 111 ± 11 μl/mg protein/5 min for M2 and M3, and 77.5 ± 11.2 μl/mg protein/5 min for M4. The uptake as the percent remaining is the ratio of the uptake volume in the presence of inhibitor to that in the absence of inhibitor (concentration, 0 μmol/liter) and is expressed as the mean ± SD from triplicate determinations.
[b] —, not tested.
[c] Delamanid metabolites M1 and M2 were incubated at 10 μmol/liter. Delamanid and M3 were incubated at 5 μmol/liter because of their low solubilities.
[d] The control was cyclosporine at 10 μmol/liter.

droxyoxazole derivative (M2) and the deamine metabolite, the (*R*)-4,5-dihydro-2-oxooxazole derivative (M4), and M2 is further hydroxylated to the (*S*)-2-imino-oxazolidin-4-one derivative (M3). All four delamanid metabolites have areas under the concentration-time curves (AUCs) close to 10% of the total AUC for all delamanid-related compounds; therefore, complete characterization of their interactions with transporters is critical for evaluating the risk of potential clinically relevant pharmacokinetic interactions with other anti-TB medications. We demonstrate that neither delamanid nor these metabolites inhibit multiple types of ABC, SLC, OATP, OAT, and OCT transporters at clinically relevant concentrations. Thus, adverse DDIs are unlikely, at least with anti-TB treatments that are substrates for these transporters.

The latest guidelines on the investigation of drug interactions authorized by the European Medicines Agency (EMA) (26) and the U.S. Food and Drug Administration (FDA) (draft) (27) focus on the ABC transporters P-gp/ABCB1 and BCRP/ABCG2, SLC transporters, the OATPs OATP1B1 and OATP1B3, the OATs OAT1 and OAT3, and the OCTs OCT1 and OCT2, which are the major drug transporters expressed in the human intestine, liver, kidney, and brain. In addition, we also tested the ABC transporter BSEP, which exports bile salts from hepatocytes.

P-gp and BCRP are located in the apical membrane of intestinal epithelial cells, where they can actively excrete a variety of structurally diverse drugs back into the lumen, thereby limiting oral absorption (7, 13). For meaningful *in vitro* evaluation of the inhibitory potency of drugs for intestinally expressed transporters, such as P-gp and BCRP, the maximum expected concentration of drugs in the intestinal lumen should be present on the apical side of enterocytes. When the test drug is orally dosed, the experimental concentration recommended by the European Medicines Agency guideline is 0.1-fold the maximum dose on one occasion/250 ml (26). However, because of its low solubility, even a single oral dose of 100 mg delamanid is not thought to reach the maximum soluble concentration in the intestine. In fact, delamanid is only slightly soluble even in buffer solutions of pH 1.2 or pH 2, which is lower than the pH of intestinal fluids. The maximum solubility drops dramatically at a higher pH, from 55 μmol/liter at pH 1.2 to 4 μmol/liter at pH 2. Thus, transport experiments at high delamanid concentrations are limited by its low solubility. In the present *in vitro* tests, the solubility of delamanid was no more than 5 μmol/liter in 1% BSA-HBSS or BSA-free HBSS; therefore, this was the maximum concentration tested as the substrate and/or inhibitor on the basis of the assumption that this concentration is close to that expected in the gastrointestinal tract after a single dose. At this concentration, delamanid was not a substrate for P-gp or BCRP (Fig. 2 and 3) and did not affect the P-gp-mediated transport of digoxin or the BCRP-mediated transport of prazosin (Table 1). Therefore, we concluded that the disposition of delamanid in humans is unlikely to be altered by inhibitors of P-gp and BCRP and that delamanid is unlikely to alter the oral availability and disposition of P-gp and BCRP substrates.

M1 at 3 μmol/liter was transported via P-gp in MDR1-expressing epithelial (LLC-PK1) cells (Fig. 2), but the clinical significance of P-gp-mediated efflux depends on the systemic concentrations of M1 in humans. The C_{max} of M1 reached 0.32 μmol/liter when delamanid (100 mg) was repeatedly dosed twice a day in patients

TABLE 6 Summary of inhibitory effects of delamanid and its metabolites on ATP-binding cassette transporters and solute carriers[a]

Transporter	IC_{50} (μmol/liter)[a]					C_{max}/IC_{50}[b]		$(50 \times C_{max,u})/IC_{50}$[b,c]	
	Delamanid	M1	M2	M3	M4	M1	M2	M1	M2
MDR1	(>5)	4.65	7.80	(>3)	(>3)	0.07	0.02	0.010	0.002
BCRP	(>5)	5.71	6.02	(>3)	(>3)	0.06	0.02	0.008	0.003
OAT1B1	(>5)	(>10)	(>10)	(>3)	(>3)	—[d]	—	—	—
OATP1B3	(>5)	(>10)	(>10)	(>3)	(>3)	—	—	—	—
OAT1	(>5)	(>10)	(>10)	(>3)	(>3)	—	—	—	—
OAT3	(>5)	(>10)	(>10)	(>3)	(>3)	—	—	—	—
OCT1	(>5)	(>10)	(>10)	(>3)	(>3)	—	—	—	—
OCT2	(>5)	(>10)	(>10)	(>3)	(>3)	—	—	—	—
BSEP	(>5)	(>10)	(>10)	(>5)	(>3)	—	—	—	—

[a] The values in parentheses represent the maximum concentration of the test compound in the inhibition study and indicate that 50% inhibition was not observed even at the maximum concentration tested.
[b] The C_{max}/IC_{50} and $(50 \times C_{max,u})/IC_{50}$ values were calculated using the C_{max} of the corresponding metabolite in human plasma after repeated administrations of delamanid at 100 mg twice a day for 56 days (22).
[c] The unbound fraction of M1 in plasma *in vitro* was determined as described previously (22), and the unbound fraction of M2 was assumed to be equivalent to that of M1.
[d] —, not applicable. C_{max}/IC_{50} and $(50 \times C_{max,u})/IC_{50}$ were not calculated for delamanid, M3, and M4 because they showed no potency against the transporters.

with MDR-TB (22). Therefore, given that the observed C_{max} is much lower than the delamanid concentrations used in the P-gp transport studies, it is possible that P-gp is involved in the disposition of M1. M1 has been found in the bile of rats receiving radiolabeled delamanid orally (not reported), although the contribution of P-gp to total biliary excretion is not known.

Regarding inhibition, the ratio of C_{max} to K_i or IC_{50} is a parameter commonly used to assess the risk of DDIs. The clinical C_{max} of M1 (0.32 μmol/liter) (22) for P-gp is substantially lower than the IC_{50} of M1 (4.65 μmol/liter) ($C_{max}/IC_{50} = 0.07$) (Table 6). Moreover, the IC_{50} of M2 (7.80 μmol/liter) is even higher than that of M1, and the C_{max} of M2 (0.12 μmol/liter) (22) is substantially lower than its IC_{50} ($C_{max}/IC_{50} = 0.02$) (Table 6). These C_{max}/IC_{50} values are relatively low compared with the biowaiver value (<0.1) that the draft guidance from the FDA recommends for performing a clinical DDI study (27). Moreover, the guidelines of EMA require a comparison of the values for $(50 \times C_{max,u})$ and IC_{50} for renal and hepatic efflux transporters in the case of systemic metabolites (26). The values of $(50 \times C_{max,u})/IC_{50}$ for M1 and M2 for P-gp are much smaller than the biowaiver value (<1) recommended by EMA (26) (Table 6). In addition, for drugs for which the unbound fraction (f_u) values are less than 0.01 because of high protein binding, both the FDA and the EMA guidelines require the assumption of an f_u equal to 0.01 to be on the safer side to avoid false-negative predictions (26, 27). For M1 ($f_u = 0.003$) and M2 (22), the $(50 \times C_{max,u})/IC_{50}$s for P-gp did not exceed 1, even if it was assumed that f_u was equal to 0.01. These findings and considerations are in line with the findings for BCRP. FDA and EMA require a comparison of the IC_{50} with the inlet maximum concentration in the liver or the expected maximum enterocyte concentration for orally administered drugs. However, in this case, because the metabolites are inhibitors, gut absorption is not applicable.

Moreover, after administration of a dose of delamanid, it was metabolized to M1 and M2 and sequentially to M4 and M3, with all metabolites being present together in the plasma. Therefore, it is conceivable that these metabolites have additive inhibitory effects. The additive effect can be estimated by the summation of the respective C_{max}/IC_{50} ratios or $(50 \times C_{max,u})/IC_{50}$ ratios of two metabolites (M1 and M2) or four metabolites (M1 and M2 plus M3 and M4, for which the IC_{50}s were not obtained). The sum of the C_{max}/IC_{50} ratios of M1 and M2 and the sum of the $(50 \times C_{max,u})/IC_{50}$ ratios of M1 and M2 did not exceed the biowaiver values (0.1 and 1, respectively), indicating that the inhibitory effect by the simultaneous presence of M1 and M2 might be negligible in a clinical setting. In addition, the C_{max} values of M3 and M4 are similar to those of M1 and M2, respectively (22). If they also have similar inhibitory potentials for P-gp and BCRP (Table 1), the sum of the C_{max}/IC_{50} ratios of the four metabolites may be close to 0.2, exceeding the FDA-recommended value of 0.1. Assessment of the maximum risk suggests a possible DDI with any of the substrates for P-gp or BCRP when the concentrations of all the metabolites occasionally reach the C_{max}. However, the effects would likely be transient. A simulation using a dynamic model would be an extremely useful method to precisely predict such information.

OATPs recognize anionic organic compounds and OCT1 recognizes cationic organic compounds at the plasma membrane of hepatocytes, and OATPs and OCT1 function in the uptake of substrates into the liver from circulating blood (7, 28, 29). OATs also interact with neutral and anionic compounds and OCT2 interacts with cationic compounds on the renal plasma membrane (7, 30), and the functions of OAT and OCTs are important for uptake into kidney cells and ultimate excretion. Hepatic elimination and renal elimination are governed by uptake ability as the initial process (28). Therefore, the transport rates for uptake into the liver via OATPs and OCT1 generally determine the overall hepatic metabolic fate of the substrate drug. We demonstrate that OATP1B1, OATP1B3, and OCT1 do not mediate a substantial uptake of delamanid or M1 (Fig. 4). These results as well as the lipophilicity of delamanid and the cationic properties of M1 strongly suggest that uptake into liver cells is more likely by passive diffusion than by active transport. Following hepatic uptake, delamanid and M1 are subjected to sequential metabolic reactions and/or biliary excretion. Therefore, it is expected that concomitant dosing with rifampin, a first-line anti-TB drug and a potent OATP inhibitor, would not alter the overall hepatic metabolic fate of delamanid.

In the present study, we did not examine transport via the renal uptake transporters OAT1, OAT3, and OCT2 because unchanged delamanid is not excreted into urine; therefore, a potential interaction via this renal route is unlikely. Neither delamanid nor any of its metabolites inhibited SLC uptake transporters, even when they were used at 5 and 10 μmol/liter, except for the inhibition of the OCT1-mediated transport of [^{14}C]metformin by M1 at 10 μmol/liter (Table 4), a concentration much higher than the clinical plasma concentration. Therefore, the potential impact of delamanid and M1 on the hepatic elimination of concomitantly administered drugs that are substrates of these transporters is likely to be minimal. Furthermore, delamanid and its metabolites had little effect on the activities of renal OATs and OCT2 (Tables 3 and 4). These results indicate that delamanid would not affect the hepatic or renal elimination of concomitantly administered substrate drugs.

Delamanid will be suitable for future use in first-line regimens. Hence, several clinical DDI studies of delamanid were conducted using the concomitant administration of delamanid with the antibiotic rifampin, isoniazid, or pyrazinamide, which make up the drug Rifater, which is used in first-line regimens. In these studies, delamanid did not change the pharmacokinetics of rifampin, isoniazid, or pyrazinamide (31). Delamanid and its metabolites have been reported to exhibit no or weak inhibition of CYP enzymes and no induction (23), and the effect of the activities of drug transporters was not noticeable in the present study. This may provide an explanation as to why there is an absence of a DDI with Rifater. The plasma concentration of delamanid was reduced only by the coadministration of a potent CYP3A inducer, rifampin (31). This occurred despite the fact that delamanid is primarily metabolized in the plasma by albumin and to a lesser extent by CYP3A (4, 25). The plasma concentration of a drug of the same class, pretomanid (PA-824), which was extensively metabolized via a combination of reductive and oxidative metabolic processes, including oxidation by CYP3A, was reduced by the coadministration of rifampin or efavirenz (32). Efavirenz is also an inducer of CYP3A, and the contribution of CYP3A to the overall metabolism of delamanid or pretomanid may increase when CYP3A is induced. On the basis of the finding that delamanid is not transported by any drug transporters, the involvement of CYP3A is likely one of the important key factors of the appearance of DDIs between the two novel antitubercular agents.

Integrase inhibitors (e.g., elvitegravir, dolutegravir), protease inhibitors (e.g., saquinavir, ritonavir), and nonnucleoside reverse transcriptase inhibitors (e.g., zidovudine) are anti-HIV agents known to interact with some transporters and induce transporter-mediated drug interactions (20, 21, 33–35). Delamanid may be used concomitantly with these agents for the treatment of TB in patients coinfected with HIV. Recent studies suggest that genetic variation in transporter genes is a significant determinant of interindividual variability in the absorption, disposition, and pharmacodynamic response to substrates, including antiviral drugs (12, 29, 36). In the present study, M1 was transported only by P-gp, while delamanid was not a substrate for any transporter. P-gp is a major determinant of both the brain distribution and urinary/biliary excretion of substrate compounds present in the blood. In the case of M1, changes in biliary excretion and the increased permeation of the BBB by other drugs could be of concern for certain P-gp genetic variants. However, M1 has several elimination pathways other than biliary excretion, such as through oxidation by CYPs and hydrolysis in the liver (22). Therefore, genetic variation effects and DDIs due to the interaction of P-gp with M1 are expected to be minimal, as long as biliary excretion occurs. Moreover, the plasma concentration of M1 increased by only 128% of that for control healthy subjects, even with concomitant use of two anti-HIV agents, lopinavir and ritonavir (400 mg and 100 mg twice a day, respectively), both of which are also potent inhibitors of P-gp and CYP3A4 (37). M1 is thought to passively permeate the BBB due to its high lipophilicity. The concentration of radioactivity in the brain containing a high proportion of M1 was reported to be higher than that in plasma when [^{14}C]delamanid was administered to rats (38). Therefore, the brain distribution of M1 is not expected to be substantially changed, even if the P-gp function is compromised by genetic variation or drugs that act as P-gp inhibitors.

Bile acids are known to be taken up into liver cells by the Na^+-taurocholate cotransporting polypeptide on the sinusoidal/basolateral membrane and then secreted into bile fluid by an efflux transporter, BSEP, on the canalicular/apical membrane (39). The vectorial summation of these fluxes determines the rate of biliary excretion. If the BSEP function is reduced by inhibitory drugs or gene mutation, intrahepatic cholestasis would eventually occur and cause hepatic toxicity. Therefore, the transport of bile acids by BSEP has an important clinical implication. However, delamanid and its metabolites had little effect on the activity of BSEP, suggesting that delamanid is suitable as a medication for the long-term treatment of TB.

In summary, delamanid ($\leq$5 μM) showed no inhibitory effects on the efflux ABC transporters P-gp, BCRP, and BSEP or on the hepatic or renal SLC transporters OATPs, OCTs, and OATs. Delamanid metabolites M1 and M2 inhibited the transport activities of P-gp and BCRP, but only at concentrations well above the C_{max} values observed after clinical administration. Other metabolites did not inhibit the transport activity of any transporter tested. Although M1 was transported through a monolayer of MDR1-expressing cells at relatively high concentrations, the plasma concentration of M1 has been reported to be minimally altered by the concomitant use of delamanid and potent inhibitors of P-gp. These *in vitro* data suggest that delamanid is unlikely to cause clinically relevant drug interactions resulting from effects on transporters mediating the absorption and/or disposition of coadministered drugs. These findings are particularly significant for TB and MDR-TB patients coinfected with HIV or with AIDS who are concomitantly treated with several anti-TB agents and anti-HIV agents.

ACKNOWLEDGMENTS

We are grateful to the many members at the ADME & Toxicology Research Institute of Sekisui Medical Co., Ltd., for their help and advice with the scientific discussion. We also thank the TB team members of Otsuka Pharmaceutical Co., Ltd., for reviewing the manuscript.

This research received no specific grant from any funding agency in the public, commercial, or not-for-profit sector.

REFERENCES

1. **World Health Organization.** 2015. Global tuberculosis report 2015. World Health Organization, Geneva, Switzerland. http://apps.who.int/iris/bitstream/10665/191102/1/9789241565059_eng.pdf.
2. **Chang KC, Yew WW.** 2013. Management of difficult multidrug-resistant tuberculosis and extensively drug-resistant tuberculosis: update 2012. Respirology **18:**8–21. http://dx.doi.org/10.1111/j.1440-1843.2012.02257.x.
3. **Sasaki H, Haraguchi Y, Itotani M, Kuroda H, Hashizume H, Tomishige T, Kawasaki M, Matsumoto M, Komatsu M, Tsubouchi H.** 2006. Synthesis and antituberculosis activity of a novel series of optically active 6-nitro-2,3-dihydroimidazo[2,1-b]oxazoles. J Med Chem **49:**7854–7860. http://dx.doi.org/10.1021/jm060957y.
4. **Matsumoto M, Hashizume H, Tomishige T, Kawasaki M, Tsubouchi H, Sasaki H, Shimokawa Y, Komatsu M.** 2006. OPC-67683, a nitro-dihydro-imidazooxazole derivative with promising action against tuberculosis in vitro and in mice. PLoS Med **3:**e466. http://dx.doi.org/10.1371/journal.pmed.0030466.
5. **Diacon AH, Dawson R, Hanekom M, Narunsky K, Venter A, Hittel N, Geiter LJ, Wells CD, Paccaly AJ, Donald PR.** 2011. Early bactericidal activity of delamanid (OPC-67683) in smear-positive pulmonary tuberculosis patients. Int J Tuberc Lung Dis **15:**949–954. http://dx.doi.org/10.5588/ijtld.10.0616.
6. **Gler MT, Skripconoka V, Sanchez-Garavito E, Xiao H, Cabrera-Rivero JL, Vargas-Vasquez DE, Gao M, Awad M, Park SK, Shim TS, Suh GY, Danilovits M, Ogata H, Kurve A, Chang J, Suzuki K, Tupasi T, Koh WJ, Seaworth B, Geiter LJ, Wells CD.** 2012. Delamanid for multidrug-resistant pulmonary tuberculosis. N Engl J Med **366:**2151–2160. http://dx.doi.org/10.1056/NEJMoa1112433.
7. **Giacomini KM, Huang SM, Tweedie DJ, Benet LZ, Brouwer KL, Chu X, Dahlin A, Evers R, Fischer V, Hillgren KM, Hoffmaster KA, Ishikawa T, Keppler D, Kim RB, Lee CA, Niemi M, Polli JW, Sugiyama Y, Swaan PW, Ware JA, Wright SH, Yee SW, Zamek-Gliszczynski MJ, Zhang L.** 2010. Membrane transporters in drug development. Nat Rev **9:**215–236. http://dx.doi.org/10.1038/nrd3028.
8. **Tsuji A.** 2006. Impact of transporter-mediated drug absorption, distribution, elimination and drug interactions in antimicrobial chemotherapy. J Infect Chemother **12:**241–250. http://dx.doi.org/10.1007/s10156-006-0478-3.
9. **Hua WJ, Hua WX.** 2014. The role of transporters in the pharmacokinetics of antibiotics. Adv Pharmacoepidemiol Drug Saf **3:**1000168. http://dx.doi.org/10.4172/2167-1052.1000168.
10. **Arakawa H, Shirasaka Y, Haga M, Nakanishi T, Tamai I.** 2012. Active intestinal absorption of fluoroquinolone antibacterial agent ciprofloxacin by organic anion transporting polypeptide, Oatp1a5. Biopharm Drug Dispos **33:**332–341. http://dx.doi.org/10.1002/bdd.1809.
11. **Alvarez AI, Pérez M, Prieto JG, Molina AJ, Real R, Merino G.** 2008. Fluoroquinolone efflux mediated by ABC transporters. J Pharm Sci **97:**3483–3493. http://dx.doi.org/10.1002/jps.21233.
12. **Burckhardt G.** 2012. Drug transport by organic anion transporters (OATs). Pharmacol Ther **136:**106–130. http://dx.doi.org/10.1016/j.pharmthera.2012.07.010.
13. **Schinkel AH, Jonker JW.** 2003. Mammalian drug efflux transporters of the ATP binding cassette (ABC) family: an overview. Adv Drug Deliv Rev **55:**3–29. http://dx.doi.org/10.1016/S0169-409X(02)00169-2.
14. **Schwarz UI, Gramatté T, Krappweis J, Oertel R, Kirch W.** 2000. P-glycoprotein inhibitor erythromycin increases oral bioavailability of talinolol in humans. Int J Clin Pharmacol Ther **38:**161–167. http://dx.doi.org/10.5414/CPP38161.
15. **Ando T, Kusuhara H, Merino G, Alvarez AI, Schinkel AH, Sugiyama Y.**

2007. Involvement of breast cancer resistance protein (ABCG2) in the biliary excretion mechanism of fluoroquinolones. Drug Metab Dispos **35:** 1873–1879. http://dx.doi.org/10.1124/dmd.107.014969.

16. **Lau YY, Huang Y, Frassetto L, Benet LZ.** 2007. Effect of OATP1B transporter inhibition on the pharmacokinetics of atorvastatin in healthy volunteers. Clin Pharmacol Ther **81:**194–204. http://dx.doi.org/10.1038/sj.clpt.6100038.
17. **Seithel A, Eberl S, Singer K, Auge D, Heinkele G, Wolf NB, Dörje F, Fromm MF, König J.** 2007. The influence of macrolide antibiotics on the uptake of organic anions and drugs mediated by OATP1B1 and OATP1B3. Drug Metab Dispos **35:**779–786. http://dx.doi.org/10.1124/dmd.106.014407.
18. **Pan X, Wang L, Grundemann D, Sweet DH.** 2013. Interaction of ethambutol with human organic cation transporters of the SLC22 family indicates potential for drug-drug interactions during antituberculosis therapy. Antimicrob Agents Chemother **57:**5053–5059. http://dx.doi.org/10.1128/AAC.01255-13.
19. **Petri N, Tannergren C, Rungstad D, Lennernäs H.** 2004. Transport characteristics of fexofenadine in the Caco-2 cell model. Pharm Res **21:** 1398–1404. http://dx.doi.org/10.1023/B:PHAM.0000036913.90332.b1.
20. **Chauvin B, Drouot S, Barrail-Tran A, Taburet AM.** 2013. Drug-drug interactions between HMG-CoA reductase inhibitors (statins) and antiviral protease inhibitors. Clin Pharmacokinet **52:**815–831. http://dx.doi.org/10.1007/s40262-013-0075-4.
21. **Minuesa G, Huber-Ruano I, Pastor-Anglada M, Koepsell H, Clotet B, Martinez-Picado J.** 2011. Drug uptake transporters in antiretroviral therapy. Pharmacol Ther **132:**268–279. http://dx.doi.org/10.1016/j.pharmthera.2011.06.007.
22. **Sasahara K, Shimokawa Y, Hirao Y, Koyama N, Kitano K, Shibata M, Umehara K.** 2015. Pharmacokinetics and metabolism of delamanid, a novel anti-tuberculosis drug, in animals and humans: importance of albumin metabolism in vivo. Drug Metab Dispos **43:**1267–1276. http://dx.doi.org/10.1124/dmd.115.064527.
23. **Shimokawa Y, Sasahara K, Yoda N, Mizuno K, Umehara K.** 2014. Delamanid does not inhibit or induce cytochrome P450 enzymes in vitro. Biol Pharm Bull **37:**1727–1735. http://dx.doi.org/10.1248/bpb.b14-00311.
24. **Meng M, Smith B, Johnston B, Carter S, Brisson J, Roth SE.** 2015. Simultaneous quantitation of delamanid (OPC-67683) and its eight metabolites in human plasma using UHPLC-MS/MS. J Chromatogr B Analyt Technol Biomed Life Sci **1002:**78–91. http://dx.doi.org/10.1016/j.jchromb.2015.07.058.
25. **Shimokawa Y, Sasahara K, Koyama N, Kitano K, Shibata M, Yoda N, Umehara K.** 2015. Metabolic mechanism of delamanid, a new anti-tuberculosis drug, in human plasma. Drug Metab Dispos **43:**1277–1283. http://dx.doi.org/10.1124/dmd.115.064550.
26. **European Medicines Agency.** 21 June 2012. Guideline on the investigation of drug interactions. European Medicines Agency, London, United Kingdom. http://www.ema.europa.eu/docs/en_GB/document_library/Scientific_guideline/2012/07/WC500129606.
27. **U.S. Department of Health and Human Services, FDA, Center for Drug Evaluation and Research.** February 2012. Guidance for industry, drug interaction studies—study design, data analysis, implications for dosing, and labeling recommendations. U.S. Department of Health and Human Services, Washington, DC. http://www.fda.gov/downloads/drugs/guidancecomplianceregulatoryinformation/guidances/ucm292362.
28. **Shitara Y, Maeda K, Ikejiri K, Yoshida K, Horie T, Sugiyama Y.** 2013. Clinical significance of organic anion transporting polypeptides (OATPs) in drug disposition: their roles in hepatic clearance and intestinal absorption. Biopharm Drug Dispos **34:**45–78. http://dx.doi.org/10.1002/bdd.1823.
29. **Fahrmayr C, Fromm MF, König J.** 2010. Hepatic OATP and OCT uptake transporters: their role for drug-drug interactions and pharmacogenetic aspects. Drug Metab Rev **42:**380–401. http://dx.doi.org/10.3109/03602530903491683.
30. **Sekine T, Miyazaki H, Endou H.** 2006. Molecular physiology of renal organic anion transporters. Am J Physiol Renal Physiol **290:**F251–F261. http://dx.doi.org/10.1152/ajprenal.00439.2004.
31. **Lewis JM, Sloan DJ.** 2015. The role of delamanid in the treatment of drug-resistant tuberculosis. Ther Clin Risk Manag **11:**779–791. http://dx.doi.org/10.2147/TCRM.S71076.
32. **Dooley KE, Luetkemeyer AF, Park JG, Allen R, Cramer Y, Murray S, Sutherland D, Aweeka F, Koletar SL, Marzan F, Bao J, Savic R, Haas DW, AIDS Clinical Trials Group A5306 Study Team.** 2014. Phase I safety, pharmacokinetics, and pharmacogenetics study of the antituberculosis drug PA-824 with concomitant lopinavir-ritonavir, efavirenz, or rifampin. Antimicrob Agents Chemother **58:**5245–5252. http://dx.doi.org/10.1128/AAC.03332-14.
33. **Griffin L, Annaert P, Brouwer KL.** 2011. Influence of drug transport proteins on the pharmacokinetics and drug interactions of HIV protease inhibitors. J Pharm Sci **100:**3636–3654. http://dx.doi.org/10.1002/jps.22655.
34. **Zembruski NC, Buchel G, Jodicke L, Herzog M, Haefeli WE, Weiss J.** 2011. Potential of novel antiretrovirals to modulate expression and function of drug transporters in vitro. J Antimicrob Chemother **66:**802–812. http://dx.doi.org/10.1093/jac/dkq501.
35. **Reese MJ, Savina PM, Generaux GT, Tracey H, Humphreys JE, Kanaoka E, Webster LO, Harmon KA, Clarke JD, Polli JW.** 2013. In vitro investigations into the roles of drug transporters and metabolizing enzymes in the disposition and drug interactions of dolutegravir, a HIV integrase inhibitor. Drug Metab Dispos **41:**353–361. http://dx.doi.org/10.1124/dmd.112.048918.
36. **Bruhn O, Cascorbi I.** 2014. Polymorphisms of the drug transporters ABCB1, ABCG2, ABCC2 and ABCC3 and their impact on drug bioavailability and clinical relevance. Expert Opin Drug Metab Toxicol **10:**1337–1354. http://dx.doi.org/10.1517/17425255.2014.952630.
37. **Paccaly A, Petersen C, Patil S, Bricmont P, Kim J, Harlin M, Wells C.** 2012. Abstr 19th Int AIDS Conf, Washington, DC, poster WERE043.
38. **Miyamoto G, Shimokawa Y, Itose M, Koga T, Hirao Y, Kashiyama E.** 2005. Abstr 45th Intersci Conf Antimicrob Agents Chemother, Washington, DC, poster F-1466.
39. **Takikawa H.** 2002. Hepatobiliary transport of bile acids and organic anions. J Hepatobiliary Pancreat Surg **9:**443–447. http://dx.doi.org/10.1007/s005340200055.
40. **Pal D, Mitra AK.** 2006. MDR- and CYP3A4-mediated drug-drug interactions. J Neuroimmune Pharmacol **1:**323–339. http://dx.doi.org/10.1007/s11481-006-9034-2.